International Journal of Nanoelectronics and Materials
IJNeaM
ISSN 198-5761 | E-ISSN 2232-1535


# Development of a Portable Gold Nanobipyramids-Based LSPR Sensor for Rapid Malathion Detection

Zarina Tukiran[a,b,*], Marlia Morsin[a,c,d,*], Nur Anis Aqilah Abdul Halim[a,c], Nur Liyana Razali[a,c], Nan Mad Sahar[c], and Suratun Nafizah[e]

[a]*Microelectronics and Nanotechnology – Shamsuddin Research Centre (MiNT-SRC), Institute for Integrated Engineering, Universiti Tun Hussein Onn Malaysia, 86400, Batu Pahat, Johor, Malaysia*
[b]*Faculty of Computer Science and Information Technology, Universiti Tun Hussein Onn Malaysia, 86400, Batu Pahat, Johor, Malaysia*
[c]*Department of Electronic Engineering, Faculty of Electrical and Electronic Engineering, Universiti Tun Hussein Onn Malaysia, 86400, Batu Pahat, Johor, Malaysia*
[d]*Institute of Nano Electronic Engineering, Universiti Malaysia Perlis, 01000 Kangar, Perlis, Malaysia*
[e]*Department of Electrical Engineering, Institut Teknologi Sumatera (ITERA), Lampung Selatan, 35365, Indonesia*
**Corresponding author. E-mail: zarin@uthm.edu.my, marlia@uthm.edu.my*

Received 1 Aug 2025, Revised 21 Jan 2026, Accepted 21 May 2026

**ABSTRACT**

Detecting pesticide residues using conventional laboratory methods is highly accurate; however, are not practical for onsite monitoring due to the requirement of complex procedures, long analysis times, and expensive equipment and maintenance. In this work, we present a portable and cost-effective sensor system for malathion detection. It is based on a localised surface plasmon resonance (LSPR) approach. The proposed system integrates gold nanobipyramids (GNBPs) as the sensing material, a SparkFun Triad Spectroscopy Sensor, and an Arduino UNO microcontroller. To monitor shifts in light wavelength in the presence of malathion, GNBPs with a surface density of approximately 69.623% and an average aspect ratio of 1.65 ± 0.06 are used. Later on, these spectral changes are captured by the spectroscopy sensor, processed by the Arduino UNO, and the LCD screen will display it in real time. The prototype is housed in a custom 3D-printed casing made from biodegradable PLA with a matte black finish to minimise stray light reflections and improve portability and ease of use. The experimental results show that the portable LSPR sensor provides a highly precise response at malathion concentrations as low as 0.5 mg/mL and offers a rapid and reliable alternative to standard laboratory techniques. The proposed device is suitable for agricultural workers as a practical tool for monitoring pesticide residues. This will support more sustainable agricultural practices, reducing environmental contamination, and lead to enhanced food safety.

**Keywords:** *Gold nanobipyramids (GNBPs), malathion detection, portable sensor, Arduino UNO, localised surface plasmon resonance (LSPR), and agricultural monitoring*

## 1. INTRODUCTION

Pesticide residues, especially organophosphate compounds such as malathion, continue to raise concern due to their harmful effects on human health and the environment. Malathion is largely used in agricultural activities; nevertheless, its persistence in the ecosystem often causes soil, crop, and water body contamination. This can often cause human health hazards to the individual through the intake of the contaminated material or through indirect contact with the contaminated material [1], [2]. Apart from the human health aspects, malathion often causes ecological imbalances in the ecosystem through the destruction of beneficial organisms such as pollinators and soil flora [3]. These are often essential for maintaining ecological balance and supporting agricultural productivity.

A well-known precision and accuracy conventional method of analysis for pesticide residues is high-performance liquid chromatography (HPLC) and gas chromatography mass spectrometry (GC MS) [4]. On the other hand, a drawback of these analysis methods is that they have a requirement for advanced equipment and a rather longer procedure, thus limiting their applicability for rapid analysis and field analysis [5]. Hence, their application in field analysis is also limited; therefore, rapid analysis and intervention of pesticide residues becomes difficult.

One of the benefits brought by the advancement in nanotechnology is the emergence of faster and more efficient sensing technologies. In this field, nanotechnology is prominent, particularly with the help of gold nanoparticles (GNPs) in detection technology. These nanoparticles work based on the principle of Localized Surface Plasmon Resonance (LSPR). Here, light is used to excite the electrons on the surface of nanoparticles, resulting in unique optical signals. However, upon binding of the target analyte, malathion, to nanoparticles, characteristic shifts in SPR signals are observed, enabling real-time detection with greater sensitivity and specificity, as reported in [6]. Of all the nanoparticle geometries, gold nanobipyramids (GNBPs) have been proven to be of particular interest because of their distinctive optical, chemical, and electrical properties in [7]. The main reason behind this is their sharp tips along with their large surface-to-volume ratio, which facilitates greater molecular adsorption, thereby increasing detection sensitivity as in [8].

Integration of GNBP-based systems with spectroscopy sensors and microcontroller-based platforms improves their use in portable detection systems. For example, the SparkFun Triad Spectroscopy Sensor can detect spectral variation across a wide wavelength range when nanoparticles are in close proximity to the target analyte molecules [9]. An inexpensive microcontroller like the Arduino UNO provides a straightforward interface through which sensor data can be interpreted and relayed in real time, allowing the user to effectively gauge malathion levels in a clear, readable, and understandable manner. The system design considers ease of use, portability, and affordability. Therefore, it would be a useful solution for fast, on-site pesticide detection and for agricultural and environmental issues [10].

This study fabricates gold nanoparticles with bipyramidal geometry as the active sensing element. The sensor is assembled with the fabricated GNBPs, a SparkFun Triad Spectroscopy Sensor, an Arduino Uno microcontroller, and an LED to enable real-time detection of malathion.

## 2. MATERIALS AND METHODS

This study has been conducted in 4 stages. Firstly, the GNBPs were fabricated and characterised as sensing materials; following this, the malathion solution was prepared and the sensor was evaluated. Next, the portable sensor casing was designed, and finally, the complete sensing hardware was implemented. The details of each stage are outlined in the following sections.

### 2.1. Fabrication and Characterisation of Gold Nanobipyramids as Sensing Material

The synthesis of GNBPs was carried out using the Seed Mediated Growth Method (SMGM) following the recipe established in our previous work [11],[12]. The materials used for this work are gold (III) chloride trihydrate ($HAuCl_4.3H_2O$), chloroplatinic acid hydrate ($H_2PtCl_4.H_2O$), hexacetyltrimethylammonium bromide ($C19H_42Br$), sodium borohydride ($NaBH_4$), and ascorbic acid ($C_6H_8O_6$) purchased from Sigma Aldrich (USA). Hydrochloric acid (HCl) and silver nitrate ($AgNO_3$) are purchased from RCI Labscan (Thailand). All the materials are diluted in deionised water (DIW) with a resistivity of 18.2 MΩ.cm.

For the characterisation, the synthesised GNBPs were tested using a UV-1800 Shimadzu Spectrophotometer, Japan, with a wavelength range of 400 – 1000 nm for optical properties, a Bruker D8 Advance X-Ray Diffractometer, Germany, with a range of 20° - 60° for structural properties, and an FESEM Joel JSM-7600, USA, with a magnification of 100000X for morphological properties.

### 2.2. Preparation of Malathion Solution and Sensor Testing

Malathion was used as the target analyte in this study. It is a commercialised pesticide produced by MAPA, registered under LRMP.R/6314. This Malathion has a concentration of 57%. In order to study the effect of concentration, the Malathion stock solution with 57% concentration was diluted to vary the Malathion solution concentration from 0.05% to 0.9% (0.5 – 9.0 mg/mL). Each Malathion concentration was prepared in a volume of 20 mL of solution.

As previously explained, GNBPs were used as a sensing material for malathion detection. There are three testing performed in this study, namely the sensitivity, stability, and repeatability. Each testing was repeated not less than five times to ensure precise results. The details of each testing are explained as follows.

#### (a) Sensitivity testing

The sensitivity of the sensor is assessed through two tests: 1) Testing towards four different medium prepared in solutions, which are 3.0 mL of pure malathion, pure GNBPs, a combined mixture of both, and 3.0 mL of deionised (DI) water as a reference. 2) Testing towards 10 different concentrations of malathions, ranging from 0.5 mL to 5.0 mL, with an interval of 0.5 mL. In this testing, all the solutions were mixed with 2.5 ml of GNBPs. This testing aims to obtain the detection limits (LoD) of the sensor as well as the response towards the different medium.

#### (b) Repeatability testing

Repeatability testing was performed to observe the response of the sensor by alternating two different medium; 2.5 mL of GNBPs mixed with 0.5 mL of malathion, and 0.5 mL of DI water in five measurement cycles. The response and recovery times are recorded to assess the sensor's reliability and consistency. The relative standard deviation (RSD) of the LSPR peak was measured to ensure the response is within the acceptable range.

#### (c) Stability testing

The final test is stability testing, which examines the sensor's performance. The test was done by monitoring the result of 3.0 mL of GNBPs mixed with 0.5 mL of malathion over 600 seconds. Any major changes is identified to check the durability of the sensor.

### 2.3. Implementation of Hardware in Sensor Setup

Based on Figure 1, it can be seen that there are two main hardware components of the portable sensor. These include a sensing module and a microcontroller unit (MCU). While the sensing module is responsible for carrying out malathion detection, the MCU is responsible for all control activities. In order to ensure user interface activities, a 20×4 I2C LCD is used. This is accompanied by a 4,000 mAh power bank.

#### *2.3.1. Sensing Module*

The sensing module integrated two key components: gold nanoparticles-based sensor and an AS7265X multispectral sensor. The gold nanoparticle-based sensor is housed within a standard optical cuvette, as illustrated in Figure 2.

The AS7265X sensor by SparkFun combines the functionality of three sensors (AS72651, AS72652, and AS72653) into a single package and offers 18 discrete spectral channels (see Figure 3 [13]). The sensors measure three different wavelength bands. The AS7261 sensor has a near-infrared (NIR) spectrum of 610-860 nm, the AS7262 sensor has a visible (Vis) spectrum of 560-940 nm, and the AS7263 sensor has an ultraviolet (UV) spectrum of 410-535 nm. The AS7265X sensor has a programmable LED electronic shutter and three LEDs for illumination. These LEDs are a white LED (5700K), a UV LED (402 nm), and an infrared LED (875 nm). The AS7265X sensor has the capability to utilize these LEDs as external light sources for enhanced detection.

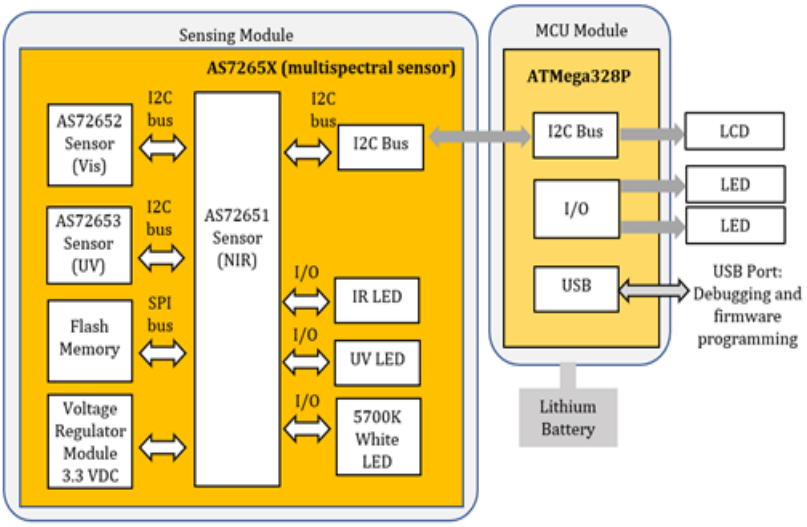


**Figure 1**. The Portable sensor hardware configuration.

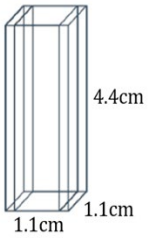


**Figure 2**. The optical cuvette for GNBPs sensing material.

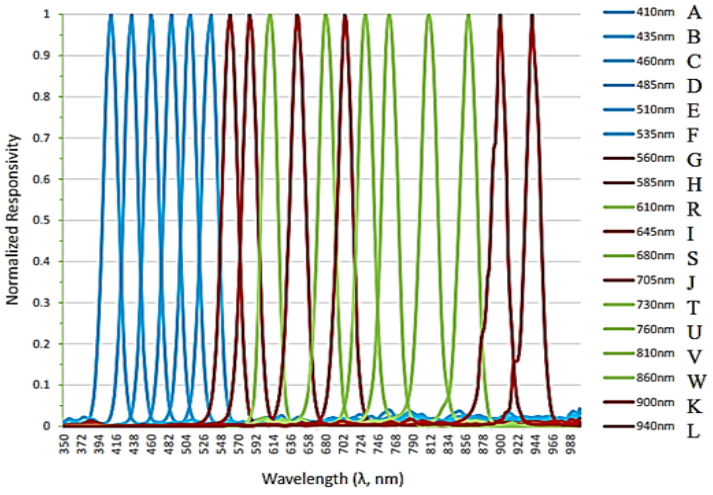


**Figure 3**. Spectral coverage of the AS7265X multispectral sensor [13].

### *2.3.2. Microcontroller Unit (MCU) Module*

The MCU module uses an 8-bit ATmega328P (Arduino) [14] as its core processing unit. In this design, the MCU acquires spectral measurements from the sensing module to detect malathion. There are two extra LEDs to supply additional external light during measurement. The system processed these results and displays them on the LCD screen in real time.

### *2.3.3. Casing Design of the Portable Sensor*

For easier portability and the application of the LSPR sensor, a customized housing made through 3D printing using polylactic acid (PLA) was used. The customized housing design in figures 4(a) to (c) was created in SketchUp. The choice of PLA was because it is biodegradable, reducing the amount of plastics in landfills. This is in line with sustainable design principles.

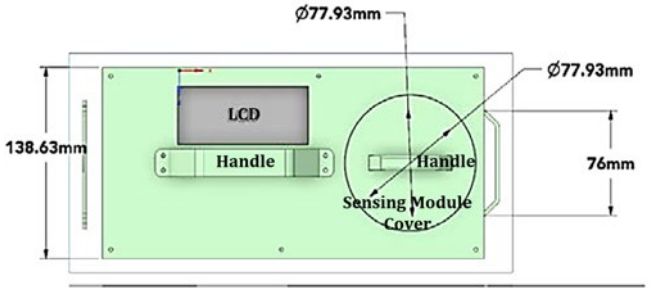


(a) Top view

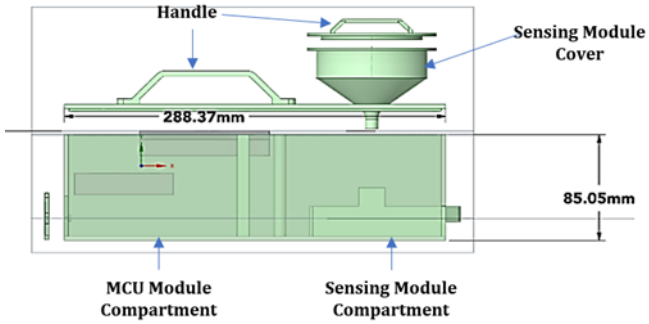


(b) Side view

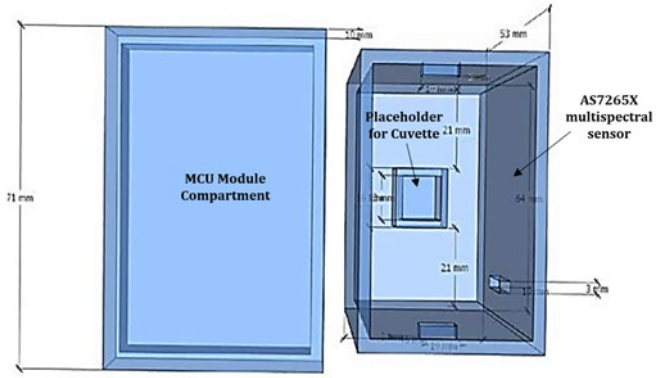


(c) Inside view

**Figure 4**. Design of the portable sensor casing.

## 3. RESULTS AND DISCUSSION

### 3.1. Results of Fabrication and Characterisation of GNBPs

In the first stage of the experiment, gold nanobipyramids (GNBPs) were successfully produced using the Seed-Mediated Growth Method (SMGM). The results from the characterization confirmed the achievement of the desired morphology and optical properties. The appearance of SPR peaks in the UV-Vis spectrum confirmed the successful production of gold nanoparticles with improved optical properties. The X-ray diffraction (XRD) spectra confirmed the crystalline structures of the particles. The results from the Field Emission Scanning Electron Microscopy (FESEM) images confirmed the uniform sizes and the desired bipyramidal shape of the nanoparticles.

The optical properties of the gold nanobipyramids (GNBPs), as can be deduced from their ultraviolet and visible (UV-Vis) absorption spectra, are shown in Figure 5. The two LSPR peaks can be identified in the spectrum. The first LSPR peak appears at 556 nm and represents the transverse plasmon mode (t-SPR), while the other LSPR peak appears at 716 nm and represents the longitudinal plasmon mode (l-SPR). The t-SPR and l-SPR peaks can be attributed to electron interactions with light along the shorter and longer axes of the nanobipyramids, respectively.

The appearance of these two distinct peaks supports the idea that GNBPs have an anisotropic shape, revealing how the incoming light interacts with the conduction electrons in response to their geometry.

From the graph, the calculated intensity ratio between the longitudinal (l-SPR) and transverse (t-SPR) plasmon bands is 2.1:1. This relatively large difference suggests that the synthesized particles are anisotropic, well-defined bipyramidal nanostructures. The graph also shows a stronger l-SPR peak than the t-SPR peak. This result supports a more longitudinal plasmonic oscillation than the transverse mode.

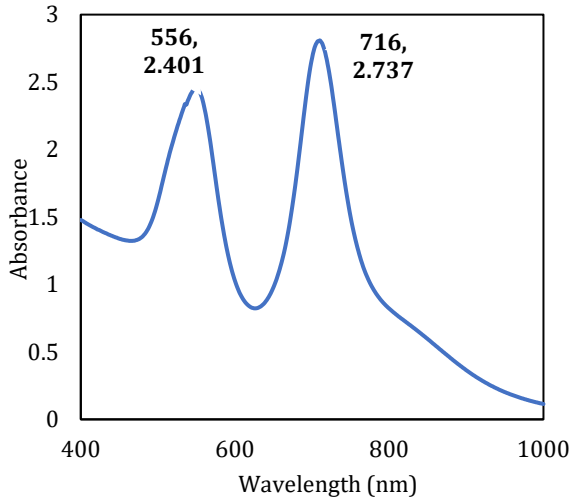


**Figure 5**. The UV-Vis absorbance spectrum of GNBPs.

Structural properties of GNBPs were determined using X-ray diffraction techniques and the results shown in Figure 6. From the results, two distinct peaks emerged at 38.17° and 51.07° for the gold particles, indexed by the (111) and (200) planes of gold (Au). This matches perfectly with the standard Inorganic Crystal Structure Database No. 98-061-1625, thus indicating the gold particles have an FCC crystal structure.

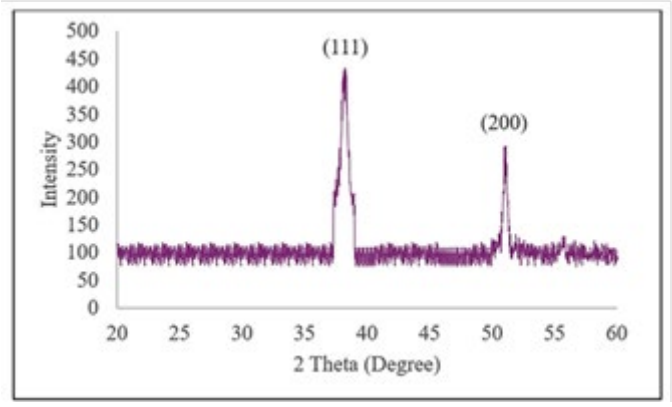


**Figure 6**. The XRD patterns of GNBPs.

The FESEM image of gold nanobipyramids (GNBPs) in Figure 7 clearly confirms the successful preparation of GNBPs with high yield. The bipyramidal structure, which is made up of two pyramidal components sharing a standard base, is clearly visible, which further confirms the accuracy of their preparation [11]. Our results show a homogeneous distribution of nanoparticle sizes, with a surface coverage of around 69.62%. The average length and width of these nanoparticles are 56.46 ± 0.81 nm and 36.36 ± 1.83 nm, respectively, with an aspect ratio of 1.65 ± 0.06. The results reflect a well-controlled synthesis process and confirm the production of structurally homogeneous GNBPs with consistent geometric properties.

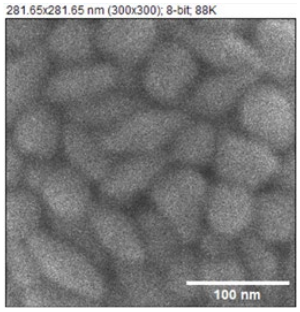


**Figure 7**. FESEM image of GNBPs.

### 3.2. Results of Sensor Testing

In this sensor testing, three main tests have been performed to assess the performance of the sensor. The tests are: sensitivity, repeatability, and stability. The changes in peak intensity and wavelength shift for LSPR responses towards the targeted analyte with different surrounding medium have been observed and analysed. The response changes are reflected in changes to the refractive index of the surrounding.

#### (a) Sensitivity testing

The sensor response towards different medium is observed and analyzed. Figure 8 shows the sensitivity result for S1) pure malathion, S2) pure GNBPs, S3) a mixture of Malathion and GNBPs, and S4) 3.0 mL of DI water as a baseline. It can be observed that the plasmon peak and wavelength shift when the surrounding medium changes.

Among all the tested samples, sample S4 with the mixture of GNBPs and 6.0 mg/mL of malathion exhibited the largest LSPR peak shift of 654 nm at a refractive index of 1.00103. The sample SI, which contains deionised water (DIW), has the lowest refractive index; therefore, only a small shift of 81 nm was observed. For the pure GNBPs sample (S2), a peak shift of 419 nm was captured, indicating their intrinsic sensitivity to changes in the surrounding medium. In contrast, the S3 sample, which contains only malathion, produced a peak shift to 546 nm, attributable to the higher refractive index of the concentrated solution.

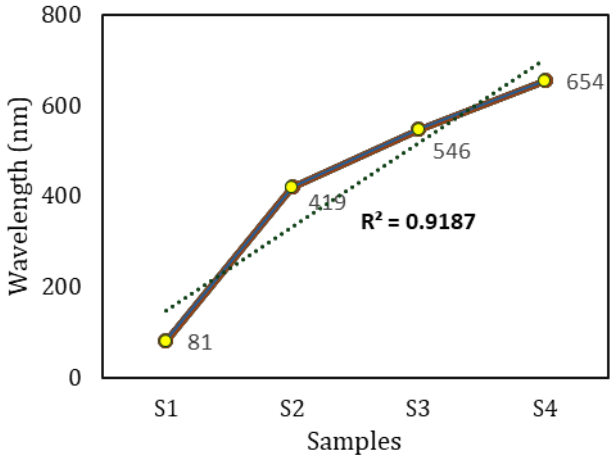


**Figure 8**. Sensitivity result for S1) 3.0 mL of DI water as a baseline, S2) pure GNBPs, S3) Malathion, and S4) 6.0 mg/mL mixture of pure GNBPs + Malathion.

The experiments were performed using different concentrations of malathion, starting from Sample 1 (S1), which was 0.5 mg/mL, $\eta$ = 1.000086, and ending with Sample 10 (S10), which was 9.0 mg/mL, $\eta$ = 1.00155, with an increase of 0.5 mg/mL for every succeeding sample. The system's responsiveness to malathion concentration is shown in Figure 9. The graph shows a linear relationship between malathion concentration and refractive index, as expected under classical refractometry principles [15]. The Lorentz-Lorenz law suggests that the increase in the solution's refractive index is directly proportional to the increase in the concentration of the solute, especially in dilute solutions [16, 17]. The increase in the LSPR peak is also related to the increase in the refractive index with increasing malathion concentration.

The results underscore the sensor's potential for agricultural monitoring and quality control, demonstrating its robustness and reliability. Malathion's lethal dose in humans has been reported to be between 0.35 and 2.0 mg/mL, and the sensor's lowest detection limit (LoD) of 0.5 mg/mL falls within this critical range been reported to be between 0.35 and 2.0 mg/mL [18], and this sensor's lowest detection limit (LoD) of 0.5 mg/mL is within this crucial range.

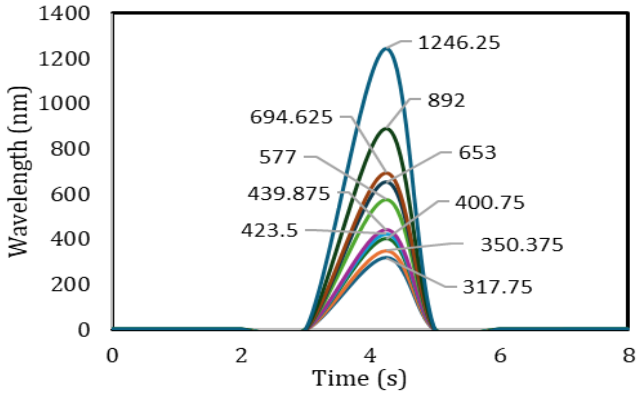


**Figure 9.** Sensitivity response across different malathion concentrations for samples S1 to S10.

### (b) Repeatability testing

For the current study, two samples were made: Sample R1 and Sample R2. Sample R1 contained gold nanobipyramids (GNBPs) in a malathion solution, while Sample R2 contained pure GNBPs for comparison purposes. The refractive index of deionized (DI) water (1.3330) was used as the standard of comparison. In addition, in order to determine the repeatability of the response of the sensor, each of the samples was subjected to five test cycles. The LSPR peaks for Sample R1 varied from 433 nm to 491 nm in each test cycle, thereby verifying the sensor's ability to measure refractive index variations in the malathion solution. However, Sample R2 showed little variation, thus verifying the stability of the response of the sensor when deionized water is used. The repeatability of the results is shown in Figure 10.

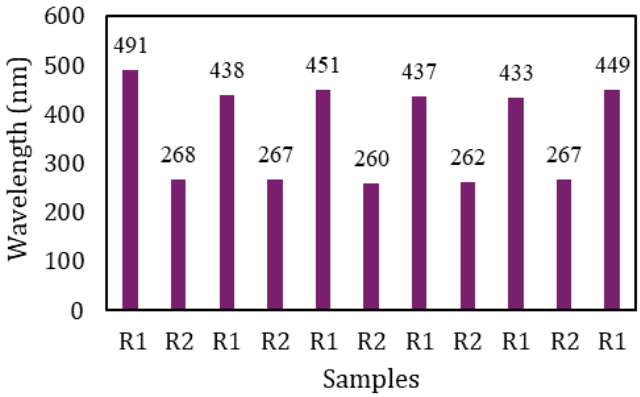


**Figure 10**. Sample R1 and Sample R2 Sensors' repeatability results.

The relative standard deviation (RSD) of the shift in the LSPR peak for Sample R1 was approximately 4.76%, indicating high consistency in the measurements. The results confirmed the sensor's reliability in measuring chemical changes and validated its potential use in environmental monitoring and safety evaluation. Overall, the results highlight the importance of consistent measurements as the starting point for further research in sensor technology to achieve accurate and reliable chemical sensing.

### (c) Stability testing

Stability testing was conducted to assess the sensor's consistency over time. For the test, a mixture of 2.5 mL of graphene-based nanomaterials (GNNPs) and 0.5 mL of malathion sample M2 was used. This mixture was then monitored for 600 seconds (10 minutes), during which the change in the LSPR peak was measured.

Figure 11 below shows the results, which indicated good stability, with little change in the reading at 261 nm. The slight variation of +1 to -1 nm is considered acceptable in this case, as it falls within the sensor's acceptable variation range. Figure 11: Stability Test Results

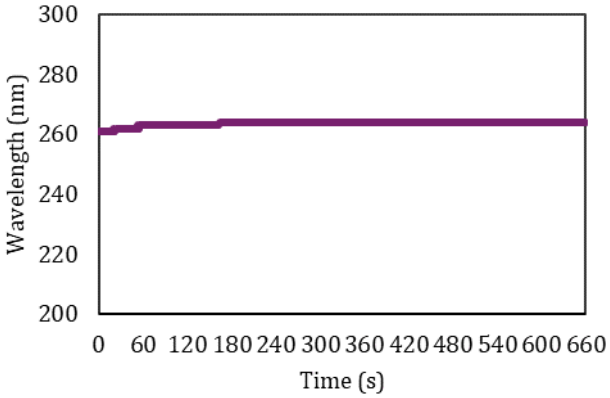


**Figure 11**. GNBPs-based sensor during 600-second continuous monitoring stability result.

### 3.3. Results of Implemented Hardware

Before integrating the entire system, functional testing was performed on the AS7265X multispectral sensor and the LCD. The testing revealed that the devices were fault-free and functioning as required. During this stage, the devices were connected to the ATmega328P microcontroller unit (MCU) to perform the necessary tasks. The functionality of the devices was observed using the integrated development environment (IDE) software via the serial monitor and plotter.

This resulted in a prototype portable sensor, as shown in Figure 12. This prototype is made up of an LCD for user interface and two handles placed at the top of the device. One of the handles is larger and helps carry the device, while the other is smaller and serves as a pull mechanism to open a cover that provides access to a compartment where the sensing module is located. When closed, it seals the device and prevents light from penetrating.

The enclosure is produced using a 3D printing technique with PLA, which has a matte black finish to suppress stray light reflections and improve the accuracy of spectral measurements. Figure 13 details the internal layout and components of the prototype.

Figure 14 illustrates the operational prototype. In the top left image, the LCD interface displays real-time status updates for the user. The top-right image captures a key moment in the detection cycle, when the integrated LEDs activate to illuminate the sample in the sensing chamber.

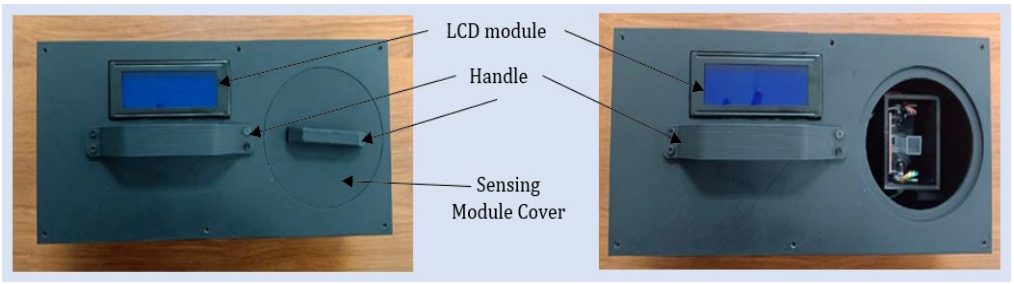


**Figure 12.** Top view of the portable sensor with the sensing module covered (left) and exposed (right).

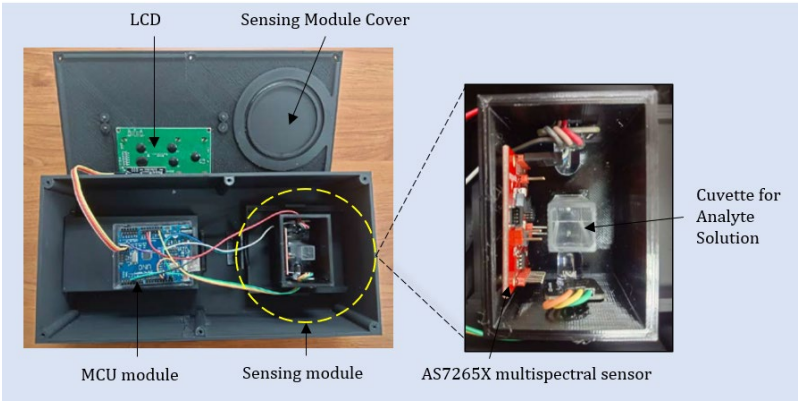


**Figure 13.** The inside view of the portable sensor; the arrangement of the sensing and MCU modules (left) and the close-up of the inside view of the sensing module (right).

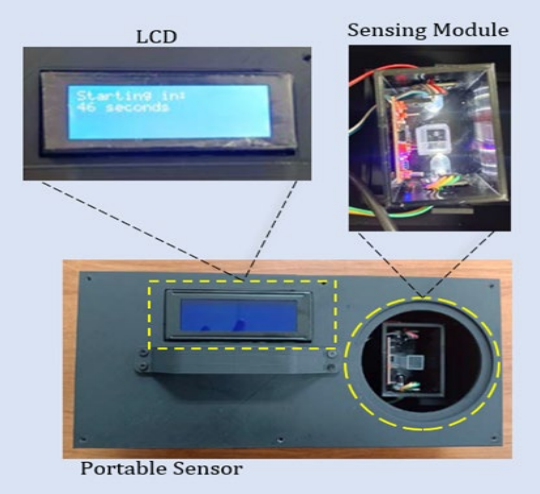


**Figure 14.** Operational states of the portable sensor prototype; (top left) the user interface via LCD, and (top right) sample illumination during detection.

### 3. 4 Benchmark Comparisons

Table 1 summaries performance metrics of this work and compares with previous work. Conventional analytical methods such as HPLC [19] and GC-MS [20] demonstrate very high sensitivity, as expected of laboratory-grade equipment. However, their practical utility for on-site testing is limited by long analysis times and a complete lack of portability.

Recent sensor technologies offer more field-deployable solutions. Electrochemical [21] and silver-nanoparticle [22] sensors show improved speed and portability with high sensitivity and very low detection limits (LODs) in the µg/L to ppb range. The GNBP-based LSPR sensor presented in this work aligns with this portable, fast-responding category. It operates in real-time and is fully portable. Its current LOD of 0.5 mg/mL, however, is significantly higher than those of the other portable sensors listed.

This finding positions the current prototype as a strong proof of concept for rapid, on-site screening. Its primary advantage lies in its operational simplicity and speed relative to lab methods. The clear focus for future development is to improve its sensitivity by lowering the LOD to be competitive with other advanced portable sensing platforms.

**Table 1** Comparison between the proposed GNBPs-based LSPR sensor and other existing sensing approaches

| Sensor | Sensitivity | LOD | Response Time | Portability | References |
|---|---|---|---|---|---|
| **HPLC** | Very high | 0.3 µg/L | Slow (minutes–hours) | Low (lab-based) | [19] |
| **GC–MS** | Very high | 2,000 µg/L | Slow (minutes–hours) | Low (lab-based) | [20] |
| **Electrochemical sensor** | High | 1 ppb (3.03 nM) | Fast (seconds–minutes) | Moderate | [21] |
| **Silver-nanoparticle sensors** | High | 0.37 µg/L | Fast | Portable | [22] |
| GNBPs-based LSPR | High | 0.5 mg/mL | Fast (real-time) | Portable | This work |

## 4. CONCLUSION

The study successfully presents a portable plasmonic device that uses bipyramidal gold nanoparticles as the sensing material for detecting malathion. The implementation of the GNBPS enhances the sensing response, with an LOD of 0.5 mg/ml. The sensor is integrated with a SparkFun Triad Spectroscopy Sensor and an Arduino Uno microcontroller for real-time monitoring and data processing. For sensor development, the eco-friendly biodegradable PLA has been used to build the string and compact sensor casing. Additionally, this portable sensor offers fast response times and cost-effectiveness to aid farmers in detecting pesticide contamination. Furthermore, this sensor offers better performance than conventional lab analysis, which incurs higher operational costs and requires skilled personnel.

In spite of its favorable results, the sensor also has several limitations, which can be remedied to improve its efficiency. In order to improve the limit of detection, the sensor material and the light source must be optimized. Furthermore, before the sensor can be used in the field, additional testing must be conducted to demonstrate its robustness and reliability. To provide accurate readings, the sensor must be tested under temperature and humidity changes, as well as potential signal interference.

In conclusion, this study presents a different, fast, real-time approach to pesticide analysis, particularly for malathion. This portable sensor is relevant to Sustainable Development Goals (SDGs) 3, 6, and 15. This helps ensure safe agricultural practices, safe food, and a healthy environment.

## ACKNOWLEDGMENTS

This research work was supported financially by the Research Management Centre (RMC), Universiti Tun Hussein Onn Malaysia, through the Tier 1 Grant (Q893). The authors thank Microelectronics & Nanotechnology-Shamsuddin Research Centre (MiNT-SRC), Universiti Tun Hussein Onn Malaysia, for the facilities.

## REFERENCES

[1] World Health Organization. Pesticides residues in food, Sep. 15, 2022. [Online]. Available: https://www.who.int/news-room/fact-sheets/detail/pesticide-residues-in-food. [Accessed: Jan. 10, 2025].

[2] B. Singh and K. Singh, "Environmental persistence of pesticides and its impact on ecological health," Journal of Environmental Research, vol. 45, no. 2, pp. 123–137, 2021.

[3] M. Qureshi et al., "Role of pesticides in disrupting soil ecosystems," Agricultural Ecosystems & Environment, vol. 187, pp. 82–91, 2020.

[4] X. Chen et al., "Advances in analytical techniques for pesticide residue detection," Analytical Chemistry Review, vol. 12, no. 3, pp. 150–175, 2019.

[5] P. Li et al., "Challenges and solutions for on-site pesticide detection," Environmental Monitoring Systems, vol. 8, no. 1, pp. 45–60, 2022.

[6] Cho, S. H., Choi, S., Suh, J. M., & Jang, H. W, "Advancements in surface plasmon resonance sensors for real-time detection of chemical analytes: sensing materials and applications," Journal of Materials Chemistry C, vol. 13, no.13, pp. 6484-6507, 2025.

[7] Wei, H., Abtahi, S. M. H., & Vikesland, P. J, "Plasmonic colorimetric and SERS sensors for environmental analysis". Environmental Science: Nano, vol. 2, no.2, pp. 120-135, 2015.

[8] S. Nafisah, M. Morsin, R. Sanudin, N. L. Razali, Z. M. Zain, and M. Djamal, "Gold nanobipyramids as LPSR sensing materials for glyphosate detection: Surface density and aspect ratio effect," IEEE Sensors Journal, vol. 22, no. 19, pp. 18479–18485, 2022

[9] SparkFun Electronics. (n.d.). Triad Spectroscopy Sensor User Guide. Available: https://www.sparkfun.com/. [Accessed: Jan. 10, 2025].

[10] A. B. D. Nandiyanto, R. Zaen, R. Oktiani, A. G. Abdullah, and L. S. Riza, "A simple, rapid analysis, portable, low-cost, and Arduino-based spectrophotometer with white LED as a light source for analyzing solution concentration," TELKOMNIKA (Telecommunication Computing Electronics and Control), vol. 16, no. 2, pp. 580–585, 2018.

[11] S. Nafisah, M. Morsin, R. Sanudin, N. L. Razali, Z. M. Zain, and M. Djamal, "Gold nanobipyramids as LPSR sensing materials for glyphosate detection: Surface density and aspect ratio effect," IEEE Sensors Journal, vol. 22, no. 19, pp. 18479–18485, 2022.

[12] S. Nafisah, M. Morsin, I. Iwantono, R. Sanudin, Z. M. Zain, L. Satria, ... and D. Mardiansyah, "Growth time dependency on the formation of gold nanobipyramids for efficient detection towards chlorpyrifos-based LPSR sensor," Optik, vol. 289, pp. 171270, 2023.

[13] ams AG, AS7265x Smart 18-Channel VIS to NIR Spectral ID 3-Sensor Chipset with Electronic Shutter, Datasheet [v1-04], Jul. 9, 2018. Available: https://look.ams-osram.com/m/76ce4c0d80cd1565/original/AS7265x-DS000612.pdf [Accessed: Jan. 9, 2025].

[14] "Arduino UNO," Components101, Jan. 9, 2025. [Online]. Available: https://components101.com/microcontrollers/arduino-uno. [Accessed: Jan. 9, 2025].

[15] N. L. Razali, W. C. Yeap, S. Nafisah, and M. Morsin, "Investigation on plasmonic based gold nanoparticles sensor for detection of malathion-toxic pesticide," in Proc. AIP Conf., vol. 2564, no. 1, p. 050016, Oct. 26, 2023, AIP Publishing LLC.

[16] S. Nafisah, M. Morsin, R. Sanudin, N. L. Razali, Z. M. Zain, and M. Djamal, "Gold nanobipyramids as LPSR sensing materials for glyphosate detection: Surface density and aspect ratio effect," IEEE Sensors Journal, vol. 22, no. 19, pp. 18479–18485, 2022.

[17] H. Kragh, "The Lorenz–Lorentz formula: Origin and early history," Substantia, vol. 2, no. 2, pp. 7–18, 2018.

[18] Agency for Toxic Substances and Disease Registry (US), Toxicological profile for malathion, Atlanta, GA, USA: ATSDR, Sep. 2, 2003. [Online]. Available: https://www.ncbi.nlm.nih.gov/books/NBK600712/.

[19] Y. Huang, T. Shi, X. Luo, H. Xiong, F. Min, Y. Chen, and M. Xie, "Determination of multi-pesticide residues in green tea with a modified QuEChERS protocol coupled to HPLC-MS/MS," Food Chemistry, vol. 275, pp. 255–264, 2019.

[20] S. Uno, A. Shintoyo, E. Kokushi, M. Yamamoto, K. Nakayama, and J. Koyama, "Gas chromatography–mass spectrometry for metabolite profiling of Japanese medaka (Oryzias latipes) juveniles exposed to malathion," Environmental Science and Pollution Research, vol. 19, no. 7, pp. 2595–2605, 2012.

[21] A. Khuntia, M. Kundu, K. Mahapatra, and A. Kumawat, "An electrochemical detection of malathion pesticide using Cu electrode and enhanced by machine learning," Chemical Engineering & Technology, p. e70036, 2025.

[22] N. Pourreza and N. Lotfizadeh, "Detection of trace malathion in vegetable, apples and water samples using silver nanoparticles immobilized in tragacanth gum and capped with citrate as a green colorimetric sensor," Journal of Food Composition and Analysis, p. 108058, 2025.